Full paper

Ultrasonic and Thermophysical Characterization of Molecular Interactions in the Benzene + Benzyl Alcohol Binary Mixture at Different Temperatures

Naveen Awasthi[1*], Sonu Dwivedi[2]

[1] Department of Chemistry, Janta College Bakewar (206124), Etawah, Uttar Pradesh, India
[2] Department of Chemistry, D.B.S. (P.G) College, Dehradun, Uttarakhand, India
* Correspondence to: nvn_awsthi@rediffmail.com

Abstract

The present study examines the Thermophysical and ultrasonic behavior of the benzene + benzyl alcohol binary mixture over the temperature range of 298.15–313.15 K. Experimental measurements of density (ρ) and ultrasonic velocity (U) were used to evaluate derived parameters such as isentropic compressibility (β_s), thermal expansion coefficient (α), isothermal compressibility (βT), internal pressure (Pi), and heat capacity ratio (γ) at different mole fractions. Theoretical estimations were performed using the Prigogine–Flory–Patterson (PFP) model, and excess properties were correlated using the Redlich–Kister polynomial equation. Percentage deviations between experimental and theoretical ultrasonic velocity and compressibility were analyzed to assess the predictive capability of the PFP model. The observed variations in thermo-acoustical parameters with temperature and composition suggest the presence of specific molecular interactions arising from polarity differences and associative tendencies of benzyl alcohol; however, these interaction mechanisms are inferred from Thermophysical behavior rather than independently confirmed. Taken together, the combined experimental–theoretical analysis provides useful insight into the non-ideal mixing behavior and structural organization of the benzene + benzyl alcohol system.
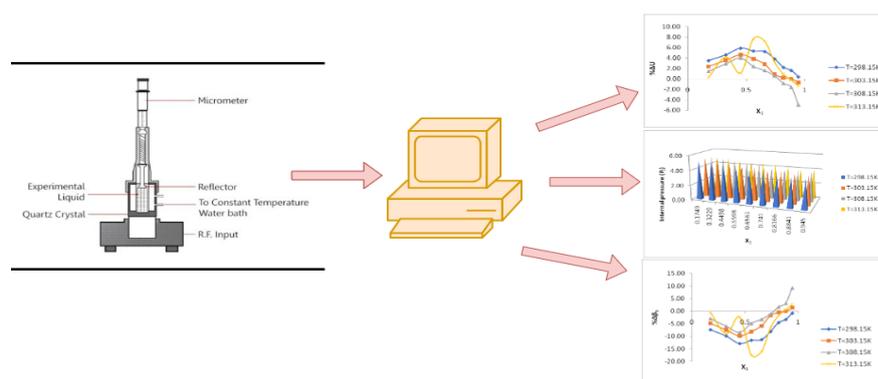
1. Introduction

Understanding the molecular interactions and thermodynamic behavior of binary liquid mixtures is essential in both academic and industrial research [1-2] as such systems often deviate from ideality due to differences in molecular size, structure, and polarity. These deviations directly influence the macroscopic properties of the mixture; such as density, ultrasonic velocity, viscosity, compressibility, and heat capacity [3], which are crucial for the design and optimization of various industrial and chemical processes. The study of such deviations not only aids in understanding intermolecular forces but also helps to predict the structure–property [4-5] relationships that govern the behavior of complex fluids. Benzene and benzyl alcohol are two widely utilized organic compounds that hold considerable significance in chemical, pharmaceutical, and materials industries [6-8]. Benzene, a non-polar aromatic hydrocarbon, is frequently employed as a reference solvent due to its well-defined structure and low dielectric constant. On the other hand, benzyl alcohol, a polar protic compound containing a hydroxyl group, exhibits strong hydrogen-bonding capability and serves as an intermediate in perfumery [9], dye manufacturing, and pharmaceutical synthesis [10]. When these two components are mixed, a variety of specific and non-specific interactions including dispersion forces, π–π stacking, and hydrogen bonding may occur, leading to complex molecular arrangements within the liquid phase. Several researchers [11-15] have investigated the Thermophysical behavior of binary liquid mixtures involving alcohols and aromatic hydrocarbons to interpret the extent of molecular association and structural organization. However, most existing reports have been limited to a single set of thermodynamic properties or narrow temperature ranges. The present study seeks to bridge this gap by offering a comprehensive Thermophysical analysis of the Benzene + Benzyl Alcohol system across multiple temperatures (298.15–313.15 K), incorporating both experimental evaluation and theoretical modeling. The experimental determination of parameters such as density (ρ) and ultrasonic velocity (U) enables the calculation of derived thermodynamic quantities including isentropic compressibility (β_s), isothermal compressibility (βT), internal pressure (Pi), thermal expansion coefficient (α), and heat capacity ratio (γ). These parameters provide meaningful insights into the nature and strength of molecular interactions within the mixture. To further quantify the non-ideality of mixing, the Redlich–Kister polynomial [16] has been employed to evaluate excess properties, while the Prigogine–Flory–Patterson (PFP) model [17-20] has been utilized to theoretically predict the behavior of the system. This integrated experimental–theoretical approach allows for a comparative evaluation of observed and predicted parameters, thereby validating the applicability of the PFP model to systems exhibiting both hydrogen-bonding and dispersive interactions. The temperature-dependent study provides a deeper understanding of how thermal agitation and molecular reorganization influence mixture behavior, which is highly relevant for solvent design, reaction engineering, and process development. Hence, this research contributes a systematic and comprehensive examination of the Benzene + Benzyl Alcohol binary mixture, offering novel insights into molecular interactions, cohesive energy density, and structure–property correlations. The findings are expected to be of significant value to both theoretical chemists and industrial practitioners, especially in the domains of solution thermodynamics, chemical process design, and materials formulation.

2. Theoretical and computational modeling

2.1 Prigogine–Flory–Patterson (PFP) model

The Prigogine–Flory–Patterson (PFP) model provides a thermodynamic framework for interpreting the behavior of non-electrolyte liquid mixtures composed of non-associated or weakly associating, γ-meric spherical chain molecules. This model assumes weak intermolecular interactions and considers deviations in thermodynamic properties primarily due to differences in molecular size, shape, and cohesive energy density. Based on the non-associated process, the PFP model allows the estimation of various characteristic parameters—namely, the characteristic pressure (P*), characteristic temperature (T*), and characteristic volume (V*), which are derived from the reduced equation of state formulated through the partition function of the system. The reduced equation of state is expressed as:

$$\frac{\tilde{P}\tilde{V}}{\tilde{T}} = \frac{\tilde{V}^{1/3}}{\tilde{V}^{1/3}-1} - \frac{1}{\tilde{V}\tilde{T}} \qquad (1)$$

$$\tilde{P} = \frac{P}{P^*} \ , \tilde{T} = \frac{T}{T^*} \ , \tilde{V} = \frac{V}{V^*} \qquad (2)$$

Here, $\tilde{P}$, $\tilde{T}$, and $\tilde{V}$ denote the reduced pressure, reduced temperature, and reduced volume, respectively. From the above relations, the thermal expansion coefficient (α) for the liquid mixture can be calculated using:

$$\alpha_{Flory} = \frac{3\left(\tilde{V}^{1/3} - 1\right)}{T\left(1 - 3\left(\tilde{V}^{1/3} - 1\right)\right)} \qquad (3)$$

A distinctive strength of the Prigogine–Flory–Patterson (PFP) model lies in its incorporation of characteristic parameters P*, T*, and V* that are derived from the intrinsic molecular structure and interaction energies of the liquid components. These parameters facilitate the use of reduced variables, enabling a comprehensive interpretation of the Thermophysical and dynamic behaviour of binary mixtures under diverse temperature and pressure conditions. Additionally, the ultrasonic velocity (U) of the system can be theoretically correlated with surface tension (σ) through the Auerbach relation, which provides a semi-empirical framework to assess molecular cohesion, compactness, and intermolecular forces governing the liquid structure.

$$U = \left(\frac{\sigma}{6.3 \times 10^{-4}\rho_{Mix}}\right)^{2/3} \qquad (4)$$

Here, σ represents the surface tension and ρ_{Mix} is the density of the binary mixture.
The surface tension of the mixture can be expressed in terms of its characteristic surface tension (σ*) and reduced surface tension (õ(v)), as proposed by Patterson and Rastogi, who extended the corresponding states theory to liquid mixtures (Eq. 5):

$$\sigma = \sigma^*\tilde{\sigma}(v) \qquad (5)$$

The characteristic surface tension (σ*) depends on the intrinsic energy and molecular size parameters of the system and is given by:

$$\sigma^* = K^{1/3}P^{*2/3}T^{*1/3} \qquad (6)$$

Where, K is the Boltzmann constant.
The reduced surface tension (õ(v)), which accounts for the dependence on reduced volume and structural factors, is evaluated using the following relation:

$$\tilde{\sigma}(v) = M\tilde{v}^{5/3} - \frac{\left(\tilde{v}^{1/3} - 1\right)}{\left(\tilde{v}^2\right)}ln\frac{\left(\tilde{v}^{1/3} - 0.5\right)}{\left(\tilde{v}^{1/3} - 1\right)} \qquad (7)$$

The internal pressure (P_i, Flory) of the mixture, which provides insight into the cohesive forces between the constituent molecules, can be evaluated theoretically as:

$$P_{i,Flory} = T \cdot \gamma_P \qquad (8)$$

Where γ_P represents the thermal pressure coefficient, which is associated with the characteristic parameters of the liquid through the relation:

$$\gamma_P = \frac{P^*}{T\tilde{V}^2} \qquad (9)$$

The isothermal compressibility $\beta_{T,Flory}$ is derived from the following expression:

$$\beta_{T,Flory} = \frac{\alpha T \, \widetilde{V}}{P^*} \qquad (10)$$

Isentropic compressibility can be calculated by well-known Newton–Laplace relation,

$$\beta_S = \left[\frac{1}{u^2 \rho_{Mix}}\right] \qquad (11)$$

The heat capacity ratio (γ) for the studied liquid mixture can be determined using the well-established thermodynamic relationship between the isothermal compressibility (βT) and the isentropic compressibility (β_s), expressed as:

$$\gamma = \frac{\beta_T}{\beta_S} \qquad (12)$$

The ratio serves as an important indicator of intermolecular interactions and energy transfer efficiency within the liquid mixture. A higher γ value suggests stronger cohesive forces and reduced energy dissipation, whereas a lower value implies increased molecular freedom and weaker interactions. Thus, the evaluation of γ offers valuable insight into the structural and dynamic behavior of the binary system over the investigated temperature range. It is important to note that the Prigogine–Flory–Patterson (PFP) model was originally developed for non-associated or weakly associated liquid systems. In the present study, benzyl alcohol possesses hydrogen-bonding capability, which is not explicitly accounted for within the PFP framework. Therefore, the application of the PFP model in this work should be regarded as a semi-empirical approximation aimed at examining overall volumetric and thermo-acoustic deviations rather than providing a complete molecular-level description. Any deviations between experimental and theoretical values may partially arise from associative interactions that are beyond the scope of the model assumptions.

3. Result and discussion

The experimentally measured ultrasonic velocity (U) and density data were used to compute a range of Thermophysical and acoustical parameters, including percentage deviation in ultrasonic velocity (%ΔU), isentropic compressibility (β_s), percentage deviation in isentropic compressibility (%$\Delta \beta_s$), thermal expansion coefficient (α), isothermal compressibility (β_T), characteristic pressure (P*), reduced volume ($\widetilde{V}$), internal pressure (P_i), and heat capacity ratio (γ). The experimental uncertainty in density measurements was estimated to be ±0.0001 g·cm⁻³, while ultrasonic velocity measurements carry an uncertainty of ±0.5 m·s⁻¹ based on instrument precision and repeatability. Consequently, percentage deviations below ~0.3% may fall within experimental uncertainty limits, whereas larger deviations reflect genuine non-ideal behavior of the mixture. The Redlich–Kister polynomial Eq. (14) was employed to fit the composition-dependent variations of excess parameters, and the corresponding coefficients (A_0–A_3) along with the standard deviation (δ) are presented in Table 1.

$$\Delta U = X_I(1 - X_1) \sum_{i=0}^{n} A_i(1 - X_1)^i \qquad (13)$$

The Redlich–Kister coefficients (A_0–A_3) exhibit systematic variation with temperature, reflecting asymmetric molecular size, polarity differences, and non-ideal mixing behavior between benzene and benzyl alcohol. The positive A_0 and A_1 coefficients indicate dominant unlike-molecule interactions at lower compositions, while negative higher-order coefficients suggest increasing deviation from ideality at higher mole fractions. The small standard deviation values (δ = 0.06–0.23) confirm the reliability of the polynomial fit and demonstrate that the Redlich–Kister equation provides a meaningful thermodynamic representation rather than a purely numerical correlation. The ultrasonic velocity (U), adiabatic compressibility (β_s), and related thermodynamic parameters of the studied binary liquid mixture were experimentally determined at four different temperatures (298.15 K, 303.15 K, 308.15 K, and 313.15 K) and are summarized in Table 2.

Table 1. Redlich–Kister polynomial coefficients and standard deviation (δ)

T/K	298.15	303.15	308.15	313.15
A0	2.70	2.83	1.74	2.51
A1	1.12	1.51	3.13	3.46
A2	-1.61	-0.59	2.34	1.89
A3	-2.63	-6.63	-11.22	-13.33
δ	0.06	0.06	0.23	0.12

The theoretical values were computed using the Flory theory, and the percentage deviations (%ΔU and %$\Delta\beta_s$) between the experimental and theoretical data were evaluated to assess the predictive capability of the model. As shown in Table 2, ultrasonic velocity decreases with increasing mole fraction of component 1 (x_1), indicating a progressive weakening of molecular interactions between unlike molecules. At 298.15 K, the maximum value of U (1526.80 m s^{-1}) is observed at lower x_1, while it decreases to 1340.50 m s^{-1} at higher mole fraction. This decline corresponds to an increase in compressibility (β_s), which is consistent with the dominance of dispersive forces and reduced structural compactness of the mixture. Although ultrasonic velocity generally decreases with increasing mole fraction and temperature, a non-monotonic behavior is observed at 313.15 K, where ultrasonic velocity exhibits a local increase at intermediate mole fractions ($x_1 \approx$ 0.55–0.65). This anomalous trend may be attributed to temporary structural rearrangements and enhanced molecular packing efficiency arising from competing dispersive and associative interactions at elevated temperature. Such behavior has been reported earlier in polar–nonpolar systems and reflects the sensitivity of ultrasonic velocity to subtle changes in molecular organization rather than a violation of the overall temperature-dependent trend. The graphical representation of %ΔU versus x_1 for all temperatures is shown in Figure 1, while Figure 2 depicts the corresponding %$\Delta\beta_s$ behavior. The %ΔU curves (Figure 1) exhibit positive deviations across most compositions, reaching a maximum at intermediate concentrations ($x_1 \approx$ 0.45–0.55), suggesting the presence of specific interactions such as dipole–dipole or hydrogen bonding between the component molecules.
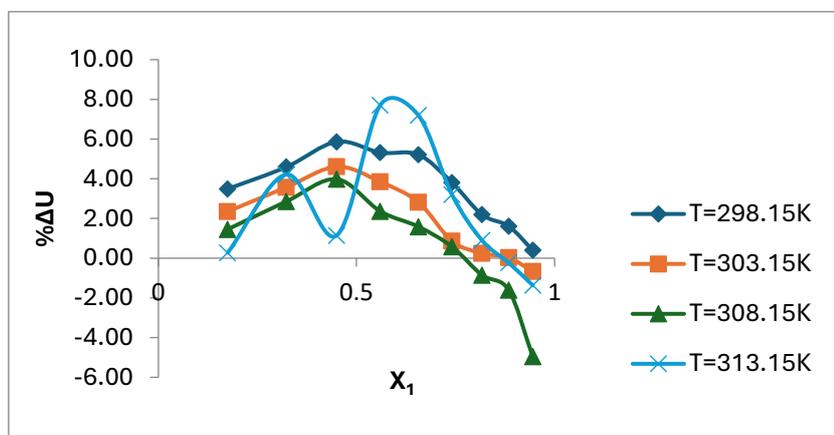
Fig. 1. Variation of %ΔU with mole fraction (x_1) at different temperatures

The deviation is most pronounced at 313.15 K, where a sharper peak indicates the temperature-induced breakdown of weak association, followed by the reorganization of molecular aggregates. Conversely, the %$\Delta\beta_s$ values (Figure 2) show negative deviations over a wide composition range, reflecting structural tightening and decreased compressibility due to effective molecular packing and interstitial accommodation between unlike species. A comparison of the experimental and theoretical ultrasonic velocities in Table 2 reveals that the Flory model tends to underestimate velocity at low x_1 and slightly overestimates at high x_1, particularly at higher temperatures. The percentage deviation in ultrasonic velocity ranges from 0.27% to 7.71%, while %$\Delta\beta_s$ varies from −0.55% to −17.39%, suggesting that the Flory approach reasonably predicts the experimental results with moderate deviations arising from non-ideal interactions. In addition to summarizing composition-dependent trends, Figure 1 directly compares experimental and theoretical

ultrasonic velocity deviations, thereby providing a visual assessment of model performance across the investigated temperature range. This comparison highlights the composition regions where the PFP model exhibits maximum deviation, complementing the numerical analysis presented in Table 2. Thermodynamic and acoustical parameters, including the thermal expansion coefficient (α), isothermal compressibility (βT), characteristic pressure (P*), reduced volume (V̌), internal pressure (Pi), and heat capacity ratio (γ), were further computed using standard thermodynamic relations, and the results are presented in Table 3.
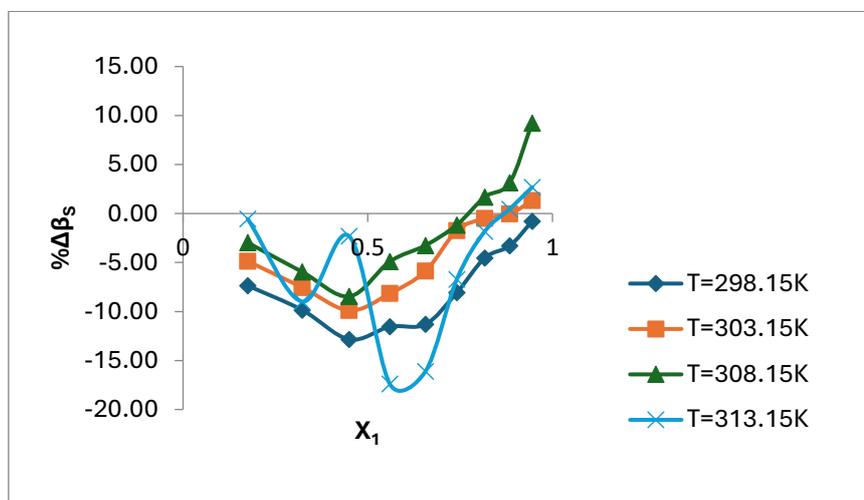

Fig. 2. Variation of $\%\Delta\beta_s$ with mole fraction (x_1) at different temperatures

The values of α and βT exhibit a systematic increase with both temperature and composition, reflecting the enhanced molecular motion and free volume in the mixture. The characteristic pressure (P*) shows a decreasing trend with temperature, signifying a reduction in molecular cohesion and structural order as thermal energy rises. Internal pressure (Pi) is a derived thermodynamic quantity influenced by density, compressibility, and thermal expansion, and therefore reflects the combined effect of several correlated parameters rather than a direct measure of interaction strength alone. The observed decrease in Pi with increasing temperature and benzene concentration indicates a reduction in cohesive energy density and structural compactness of the mixture. These trends should be interpreted qualitatively as indicative of weakening intermolecular cohesion rather than as a direct quantification of specific interaction mechanisms. Furthermore, the variation of internal pressure (Pi) with mole fraction and temperature is illustrated in Figure 3. The graph clearly shows that Pi decreases with increasing temperature and mole fraction, confirming that the strength of molecular interactions diminishes as thermal energy rises. The systematic decrease of internal pressure with temperature and concentration verifies the structure-breaking nature of the mixture, influenced by thermal expansion and the reduction of free energy of cohesion. Such a behavior typically indicates the predominance of dispersive and weak polar interactions in the binary system, reinforcing the non-ideal mixing pattern derived from ultrasonic and thermodynamic analyses. The heat capacity ratio (γ) increases slightly with composition and temperature, ranging between 1.30 and 1.55, which confirms the presence of weak associative interactions rather than strong hydrogen bonding. These variations support the existence of a transition from structure-making to structure-breaking behavior with the increase in temperature, a characteristic of partially miscible or polar–nonpolar binary systems. The heat capacity ratio (γ) increases slightly with benzene concentration, reflecting an enhanced degree of freedom due to the disruption of the hydrogen-bonded network of benzyl alcohol. Similarly, the increase in thermal expansion coefficient (α) and isothermal compressibility (βT) with temperature demonstrates the expected thermal loosening of intermolecular contacts.

$$\delta = \sqrt{\frac{\left(\sum_{i=1}^{n} \eta_{Exp} - \eta_{Theo}\right)^{1/2}}{n - p}} \qquad (14)$$

Theoretical evaluations were performed using the Prigogine–Flory–Patterson (PFP) model, which accounts for size and shape differences between unlike molecules. The model provided satisfactory agreement with

the experimental excess thermodynamic functions, confirming its applicability for polar–nonpolar mixtures such as Benzene + Benzyl Alcohol. The deviation between theoretical and experimental data may be attributed to specific hydrogen bonding effects not fully captured by the PFP framework.
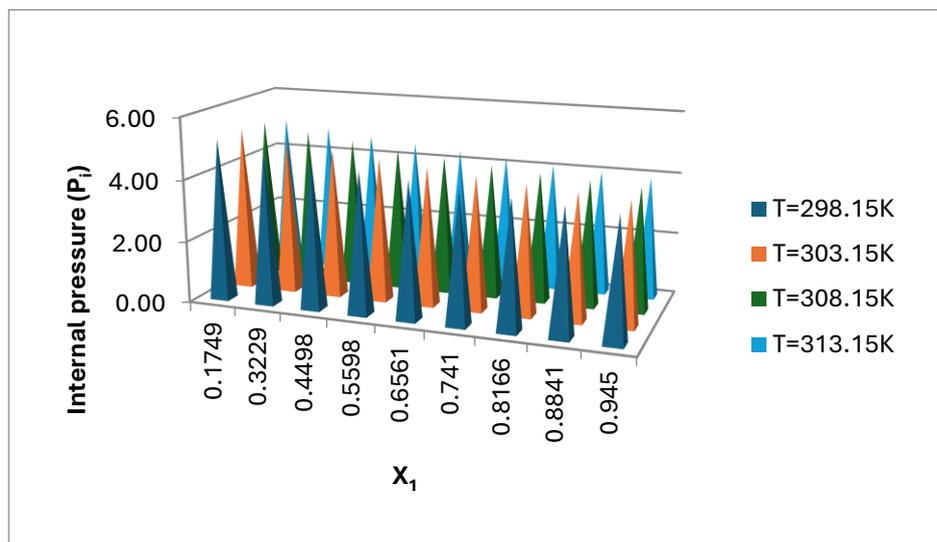

Fig. 3. Variation of internal pressure (Pi) with mole fraction (x_1) at different temperatures

Table 2. Experimental and Theoretical Evaluation of Ultrasonic and Compressibility Parameters of the Binary Mixture at Different Temperatures

X_1	ρ (g/cc)	U_{Exp}	$\beta s_{(Exp)}X10^{12}$	U_{Flory}	$\beta s_{(Theo)}X10^{12}$	%ΔU	%$\Delta \beta_s$
			T=298.15K				
0.1749	1.0008	1526.80	428.64	1473.54	460.18	3.49	-7.36
0.3229	0.9935	1502.00	446.16	1433.03	490.14	4.59	-9.86
0.4498	0.9825	1489.80	458.58	1402.46	517.47	5.86	-12.84
0.5598	0.9601	1465.80	484.77	1387.85	540.75	5.32	-11.55
0.6561	0.9445	1446.30	506.15	1370.87	563.39	5.22	-11.31
0.741	0.9236	1416.50	539.61	1362.59	583.16	3.81	-8.07
0.8166	0.9001	1390.50	574.60	1359.99	600.68	2.19	-4.54
0.8841	0.8935	1365.10	600.59	1343.11	620.42	1.61	-3.30
0.945	0.8801	1340.50	632.32	1335.18	637.37	0.40	-0.80
			T=303.15K				
0.1749	0.9998	1505.70	441.17	1470.33	462.65	2.35	-4.87
0.3229	0.9874	1489.40	456.55	1436.22	490.98	3.57	-7.54
0.4498	0.9754	1475.80	470.72	1407.84	517.26	4.61	-9.89
0.5598	0.9564	1446.80	499.51	1391.13	540.29	3.85	-8.16
0.6561	0.9354	1420.50	529.81	1380.47	560.98	2.82	-5.88
0.741	0.9002	1399.80	566.93	1387.77	576.80	0.86	-1.74
0.8166	0.8897	1376.50	593.20	1373.08	596.16	0.25	-0.50
0.8841	0.8845	1355.80	615.05	1355.48	615.34	0.02	-0.05
0.945	0.8789	1331.50	641.77	1340.37	633.30	-0.67	1.32
			T=308.15K				
0.1749	0.9875	1489.20	456.62	1467.56	470.19	1.45	-2.97
0.3229	0.9756	1476.20	470.37	1434.05	498.43	2.86	-5.97

0.4498	0.9632	1465.30	483.54	1407.01	524.44	3.98	-8.46
0.5598	0.9426	1426.50	521.35	1392.80	546.89	2.36	-4.90
0.6561	0.9254	1401.50	550.15	1379.24	568.05	1.59	-3.25
0.741	0.8992	1386.20	578.75	1378.21	585.48	0.58	-1.16
0.8166	0.8745	1367.20	611.75	1378.86	601.45	-0.85	1.68
0.8841	0.8645	1345.20	639.24	1366.76	619.23	-1.60	3.13
0.945	0.8566	1290.50	700.98	1354.49	636.31	-4.96	9.23
			T=313.15K				
0.1749	0.9745	1442.30	493.30	1438.34	496.02	0.27	-0.55
0.3229	0.9683	1466.30	480.34	1404.54	523.51	4.21	-8.99
0.4498	0.9512	1402.50	534.47	1386.50	546.87	1.14	-2.32
0.5598	0.9354	1485.90	484.20	1371.40	568.42	7.71	-17.39
0.6561	0.9102	1475.30	504.78	1369.12	586.11	7.20	-16.11
0.741	0.8754	1425.80	561.92	1380.18	599.68	3.20	-6.72
0.8166	0.8563	1390.50	603.99	1377.95	615.05	0.90	-1.83
0.8841	0.8365	1375.80	631.57	1378.95	628.70	-0.23	0.46
0.945	0.8236	1355.80	660.53	1374.39	642.78	-1.37	2.69

Table 3. Thermal expansion coefficient (α), Isothermal compressibility (βT), Characteristic pressure (P*), Reduced volume $(\widetilde{V})$, Internal pressure (Pi) and heat capacity ratio (ϒ) of binary system at different temperatures

X1	α X 10³	βT X10¹²	P*	$\widetilde{V}$	P_i	ϒ
			T=298.15K			
0.1749	1.05	59.86	8.27	1.26	5.23	1.30
0.3229	1.08	64.62	7.95	1.26	4.98	1.40
0.4498	1.10	69.11	7.67	1.27	4.77	1.41
0.5598	1.13	73.36	7.43	1.27	4.58	1.42
0.6561	1.15	77.38	7.21	1.28	4.42	1.43
0.741	1.16	81.18	7.01	1.28	4.28	1.44
0.8166	1.18	84.80	6.83	1.28	4.15	1.45
0.8841	1.19	88.22	6.67	1.29	4.03	1.47
0.945	1.21	91.49	6.53	1.29	3.93	1.47
			T=303.15K			
0.1749	1.06	60.84	8.38	1.26	5.26	1.32
0.3229	1.08	65.53	8.07	1.27	5.01	1.42
0.4498	1.11	69.94	7.79	1.27	4.81	1.42
0.5598	1.13	74.10	7.55	1.28	4.62	1.43
0.6561	1.15	78.03	7.33	1.28	4.47	1.44
0.741	1.17	81.74	7.14	1.28	4.33	1.46
0.8166	1.18	85.26	6.96	1.29	4.20	1.48
0.8841	1.20	88.59	6.81	1.29	4.09	1.49
0.945	1.21	91.75	6.67	1.29	3.99	1.49
			T=308.15K			
0.1749	1.07	62.88	8.41	1.27	5.23	1.34
0.3229	1.10	67.63	8.10	1.27	4.99	1.44
0.4498	1.12	72.09	7.83	1.28	4.79	1.45

0.5598	1.14	76.29	7.59	1.28	4.61	1.45
0.6561	1.16	80.25	7.38	1.29	4.45	1.47
0.741	1.18	83.99	7.19	1.29	4.32	1.48
0.8166	1.19	87.54	7.02	1.29	4.20	1.50
0.8841	1.21	90.89	6.86	1.30	4.09	1.51
0.945	1.22	94.08	6.72	1.30	3.99	1.52
		T=313.15K				
0.1749	1.09	67.85	8.24	1.28	5.05	1.37
0.3229	1.12	72.43	7.97	1.28	4.84	1.46
0.4498	1.14	76.72	7.73	1.29	4.66	1.47
0.5598	1.16	80.73	7.52	1.29	4.51	1.48
0.6561	1.18	84.51	7.33	1.29	4.37	1.49
0.741	1.19	88.05	7.16	1.30	4.25	1.50
0.8166	1.21	91.40	7.00	1.30	4.14	1.52
0.8841	1.22	94.56	6.86	1.30	4.04	1.54
0.945	1.23	97.55	6.74	1.31	3.96	1.55

4. Conclusion

On the basis of above discussion it can be concluded that the present ultrasonic and Thermophysical investigation confirms the non-ideal mixing behavior of the benzene + benzyl alcohol system over the temperature range 298.15–313.15 K. Variations in ultrasonic velocity, compressibility, internal pressure, and heat capacity ratio with temperature and composition suggest the presence of weak associative and dispersive interactions, inferred from Thermophysical responses. The Prigogine–Flory–Patterson model provides reasonable predictive capability, although deviations arise due to associative effects not explicitly included in the model. Collectively, the study demonstrates the effectiveness of ultrasonic techniques combined with thermodynamic modeling for qualitative assessment of molecular interactions in polar–nonpolar binary liquid mixtures.

Acknowledgements

References

[1] M. Rani and S. Maken, "Thermodynamics of molecular interactions in binary mixtures containing associated liquids," *Korean J. Chem. Eng.*, vol. 30, no. 8, pp. 1636–1643, 2013, doi: 10.1007/s11814-013-0116-5.

[2] A. Ali and A. K. Nain, "Ultrasonic study of molecular interaction in binary liquid mixtures at 30 °C," *Pramana*, vol. 58, no. 4, pp. 695–701, 2002, doi: 10.1007/s12043-002-0068-7.

[3] R. Kumar, S. Jayakumar, and V. Kannappan, "Study of molecular interactions in binary liquid mixtures," *Indian J. Pure Appl. Phys.*, vol. 46, no. 3, pp. 169–175, 2008.

[4] N. Srivastava, B. K. Rathour, and S. Singh, "Ultrasonic and thermodynamical study of molecular interactions in binary liquid mixtures at different temperatures," *Russ. J. Phys. Chem. A*, vol. 96, no. 1, pp. 15–26, 2022, doi: 10.1134/S0036024422010068.

[5] K. Narendra, C. Srinivasu, and P. Narayanamurthy, "Experimental and theoretical ultrasonic velocities of binary liquid mixtures at temperatures (303.15–318.15) K—comparative study," *Pak. J. Sci. Ind. Res. A Phys. Sci.*, vol. 55, no. 2, pp. 59–67, 2012.

[6] S. K. Ritter, "Industrial benzene use and environmental sustainability," *J. Cleaner Prod.*, vol. 267, p. 121615, 2020, doi: 10.1016/j.jclepro.2020.121615.

[7] M. J. López-Muñoz, M. Sánchez-Polo, and J. Rivera-Utrilla, "Solvent applications and environmental impact of aromatic hydrocarbons," *Chemosphere*, vol. 283, p. 132290, 2021, doi: 10.1016/j.chemosphere.2021.132290.

[8] F. Yang, X. Wang, and Z. Li, "Benzyl alcohol as a green solvent and industrial intermediate," *Ind. Crops Prod.*, vol. 140, p. 111587, 2019, doi: 10.1016/j.indcrop.2019.111587.

[9] H. J. Lee and D. H. Kang, "Fragrance and solvent roles of benzyl alcohol in industrial systems," *ACS Omega*, vol. 6, no. 19, pp. 12654–12663, 2021, doi: 10.1021/acsomega.1c01932.

[10] M. McMahon, R. Patel, and G. Singh, "Pharmaceutical and preservative applications of benzyl alcohol," *Int. J. Pharm.*, vol. 580, p. 119162, 2020, doi: 10.1016/j.ijpharm.2020.119162.

[11] J. D. Pandey, K. K. Tiwari, and V. S. Rupali Sethi, "Temperature dependent studies of thermodynamic properties of three binary systems using density and ultrasonic velocity data," *J. Pure Appl. Ultrason.*, vol. 34, pp. 41–48, 2012.

[12] J. D. Pandey, A. K. Shukla, N. Tripathi, and G. P. Dubey, "Internal pressure, ultrasonic velocity and viscosity of multicomponent liquid systems," *Pramana*, vol. 40, no. 2, pp. 81–87, 1993, doi: 10.1007/BF02845256.

[13] R. K. Shukla, A. Kumar, N. Awasthi, U. Srivastava, and K. Srivastava, "Speed of sound and isentropic compressibility of benzene with aromatic liquids from various models in the temperature range 298.15–313.15 K," *Arab. J. Chem.*, vol. 10, no. 7, pp. 895–905, 2017, doi: 10.1016/j.arabjc.2015.02.010.

[14] S. Panda, "Molecular interaction study of binary liquid solutions using ultrasonic technique," *Recent Innov. Chem. Eng.*, vol. 15, no. 2, pp. 138–146, 2022, doi: 10.2174/2405520415666210817123843.

[15] A. Sirohi *et al.*, "Estimation of ultrasonic velocity, density, internal pressure, and thermophysical parameters of ionic liquid mixtures: Application of Flory's statistical theory," *ACS Omega*, vol. 9, no. 17, pp. 19363–19377, 2024, doi: 10.1021/acsomega.4c00321.

[16] O. Redlich and A. T. Kister, "Algebraic representation of thermodynamic properties and the classification of solutions," *Ind. Eng. Chem.*, vol. 40, no. 2, pp. 345–348, 1948, doi: 10.1021/ie50458a036.

[17] A. Abe and P. J. Flory, "The thermodynamic properties of mixtures of small, nonpolar molecules," *J. Am. Chem. Soc.*, vol. 82, pp. 1838–1846, 1960, doi: 10.1021/ja01492a018.

[18] I. Prigogine and L. Saraga, "Test of monolayer model for surface tension of simple liquids," *J. Chem. Phys.*, vol. 20, pp. 399–407, 1952, doi: 10.1063/1.1700467.

[19] P. J. Flory, "Statistical thermodynamics of liquid mixtures," *J. Am. Chem. Soc.*, vol. 87, no. 9, pp. 1833–1838, 1965, doi: 10.1021/ja01087a001.

[20] P. J. Flory, R. A. Orwoll, and A. Vrij, "Statistical thermodynamics of chain molecule liquids. II. Liquid mixtures of normal paraffin hydrocarbons," *J. Am. Chem. Soc.*, vol. 86, no. 17, pp. 3515–3520, 1964, doi: 10.1021/ja01072a021.